# Formation of Two-Dimensional Nanomaterials of Boron Carbides

**Fang-Fang Xu* and Yoshio Bando**

*Advance Materials Laboratory, National Institute for Materials Science, Namiki 1-1, Tsukuba, Ibaraki 305-0044, Japan*

*Received: December 1, 2003; In Final Form: April 6, 2004*

A simple chemical vapor deposition in a graphite crucible was employed in the development of two-dimensional nanomaterials of boron carbide. The sole starting material was $B_2O_3$ powder, and the deposition was undertaken on a chemically and thermally stable insulating template, graphitic boron nitride. The majority of the boron carbide products ($B_4C$ structure, $R\bar{3}m$) exhibit a beltlike morphology with lateral dimensions of 5−10 $\mu$m (in width) and 50−100 $\mu$m (in length), while the thickness is in the nanoscale range (20−100 nm). Transmission electron microscopy revealed a strong dependence of growth morphology on the number ($n$) of different {1,−1,−1} surfaces appearing during the crystal growth. The dimensionality of the boron carbide crystallites can be described by $(3 - n)$; for example, the appearance of a sole ($n = 1$) {1,−1,−1} surface leads to a two-dimensional material while zero-dimensional particles, i.e., icosahedral quasicrystals, appear when $n = 3$. Growth morphology can possibly be controlled via controlling the temperature and the vapor pressure of the starting source.

## Introduction

Boron carbide, a lightweight refractory semiconductor, is the third hardest material on earth following diamond and cubic boron nitride (BN) but with the advantage of being stable to a very high temperature. This, along with many other outstanding physicochemical properties including high strength and Young's modulus, high capture section for neutrons, and attractive high-temperature thermoelectric properties, expedites its being a promising material that has been extensively studied in the past few decades.[1−4] Recently, development of boron carbide nanomaterials has attracted a wide range of research interest. Some one-dimensional (1D) nanostructures including nanowires, nanonecklaces, and nanosprings have been reported.[5−10] Such morphological tailoring character for boron carbide is apparently advantageous over diamond and cubic BN for which no one-dimensional nanostructures have been observed. High surface/volume ratios in nanomaterials are supposed to result in the enhancement of some properties. Therefore, boron carbide nanomaterials have promising application potentials in, for example, wear-resistant ceramics for usage in extreme conditions, a neutron absorbent in the nuclear industry, and high-temperature thermoelectric energy conversion.

In contrast to a variety of zero-dimensional (0D) and 1D nanomaterials based on the $B_4C$ structure, a two-dimensional (2D) nanomaterial, e.g., nanobelt or nanosheet, has not yet been observed in boron carbide compounds. Here, we report the development of boron carbide nanosheets via a simple high-temperature chemical vapor deposition (CVD) starting with $B_2O_3$ powder and C from the crucible. Unlike the 1D nanomaterials of boron carbide, which were synthesized either with an attendance of metal catalysts (e.g., Co, Ni, and Fe)[9] or on a porous semiconductor templates (e.g., $Al_2O_3$),[8] the present growth of 2D nanomaterials was performed on a flat insulating template, i.e., graphitic boron nitride. By the chemical inertness and thermal stability of BN, no kinematical elements are supposed to govern the growth morphology of boron carbide. The possible formation mechanism for sheet morphology is discussed.

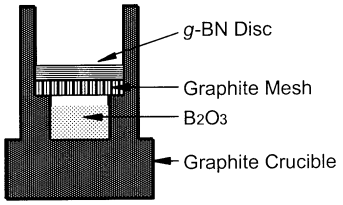


**Figure 1.** Schematic diagram of the crucible setup used in the present synthesis of boron carbide 2D nanomaterials.

## Experimental Section

A sole starting powder, $B_2O_3$ (99.99% purity), was placed into a cylindrical graphite crucible capped with a graphite mesh and a graphitic BN (g-BN) thin disk (Figure 1). The crucible was then inserted in a high-frequency (21 kHz) induction furnace JHF-VFX 110QZ (JEOL) and heated within 15 min to 1950 °C and maintained for 1 h. A fine product with metallic luster was obtained on the BN template.

The deposits were characterized by X-ray diffraction (XRD) and observed by scanning electron microscopy (SEM, JSM-6700F) and transmission electron microscopy (TEM, JEM-3000F). Chemical composition was analyzed by a Gatan DigiPEELS 766 electron energy loss spectrometer (EELS).

## Results and Discussion

The XRD spectrum of the present material consists of reflection peaks arising from two phases, i.e., $B_4C$-based crystal ($R\bar{3}m$) with strong (104) and (021) peaks (JCPDS file: 35-0798) and g-BN from the template. Apart from rodlike and polygonal particles, the majority of the as-obtained boron carbide crystallites show a beltlike morphology with a high two-dimensionality (Figure 2). The average width and length of these boron

* To whom correspondence should be addressed. Fax: +81-29-851-6280. E-mail: XU.Fangfang@nims.go.jp.

10.1021/jp037669n CCC: $27.50 
Published on Web 05/06/2004

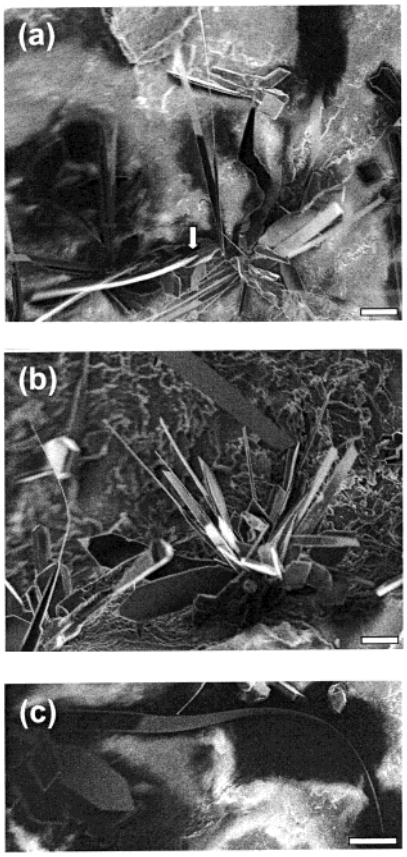


**Figure 2.** SEM images of the as-obtained products: (a, b) agglomerates of beltlike boron carbide nanomaterials; (c) a candidate of the longest belts. Scale bars: 10 $\mu$m.

carbide belts range are 5−10 and 50−100 $\mu$m, respectively. The highest length/width ratio is found to be over 20. The morphological anisotropy is further emphasized by the ultrasmall thickness, amounting to only decades to a hundred of nanometers. The thinnest sheet displays a thickness around 20 nm, as estimated from the plasmon excitation at low-loss region in an EEL spectrum (Figure 3c). The ultrathin sheets made them bend (Figure 2b,c) and appear transparent under the transmission electron microscope (Figure 3a). The straight boundaries and homogeneous image contrast indicate well-defined growth direction and boundary planes. Though these boron carbide 2D crystallites have a consistent $B_4C$-based crystal structure, the chemical composition may vary somewhat among different crystallites. At any rate, no relation between the dimensionality and the composition is observed. Figure 3c illustrates the EEL spectrum from the sheet in Figure 3a. Examination of EEL spectra acquired in a wide range of energy loss excludes possible introduction of N and/or O atoms into the structure. EELS quantification indicates a B/C atomic ratio of 5−8 for the present boron carbide sheets. The carbon in the composition must have come from the graphite crucible.

Identification of growth faces and directions of a 1D or 2D nanomaterial requires full knowledge of the crystal structures of the concerned material and comprehensive TEM operation. The surface and orientation indices apparently appearing in a TEM observation may not refer to the true geometry, behind which the real ones could only be obtained via specimen tilting. Especially for a crystal having other than a cubic symmetry, a view direction in which a good diffraction pattern appears is usually not perpendicular to the sheet surface or the fiber axis. In the present TEM observation, the most frequently obtained zone axis is $\langle 1,-1,-1\rangle$ (Figure 3) via a specimen tilting around

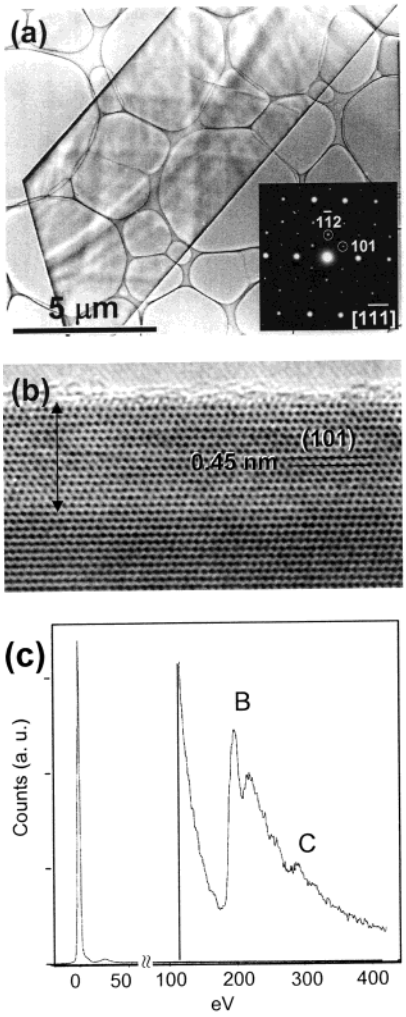


**Figure 3.** Structure and composition of boron carbide 2D nanomaterial: (a) TEM image of an individual beltlike nanobelt and its diffraction pattern (inset); (b) [1,−1,−1]-projected high-resolution TEM image of the side surface region in (a); (c) EEL spectrum at low-loss (0−50 eV) and core-loss (B K-edge at 188 eV and C K-edge at 284 eV) regions.

30° from the horizontal placement of the specimen grid. Among the close-packed planes in the $B_4C$ structure, the normals of three crystallographic faces lie close to the $\langle 1,-1,-1\rangle$ directions. They are $\{0,1,2\}$ by ∼42° to $\langle 1,-1,-1\rangle$, $\{0,0,1\}$ by ∼39°, and $\{1,-1,-1\}$ by ∼29°. By notation of tilting limit of ±20° for the microscope, the most possible sheet surface is the $\{1,-1,-1\}$, the closest packed plane in $B_4C$. This will be further documented by the experimental observations and discussions below. In an arbitrarily defined [1,−1,−1]-projected lattice image (Figure 3b) of a boron carbide nanobelt, we find that the (1,0,1) plane is parallel to the elongating direction. Then the growth direction for a belt shape can be derived, which is simply the zone axis determined by the (1,−1,−1) sheet plane and an observed parallel plane, i.e., (1,0,1). We obtain a growth direction along the [1,2,−1], which is the one belonging to the $\langle 1,-1,-1\rangle$ orientation group. Therefore, the boron carbide nanobelts display a $\{1,-1,-1\}$ sheet surface and orient along $\langle 1,2,-1\rangle$. It should be emphasized here that the (1,0,1) plane is not the side surface of the observed nanobelt, though it appears parallel to the elongating direction in this view direction, i.e., [1,−1,−1]. We note the nonhomogeneity in image contrast within a certain width from the straight boundary (as indicated by a line with arrows at both ends), implying changes in thickness at the peripheral region. Thus, the boundary face must be oblique

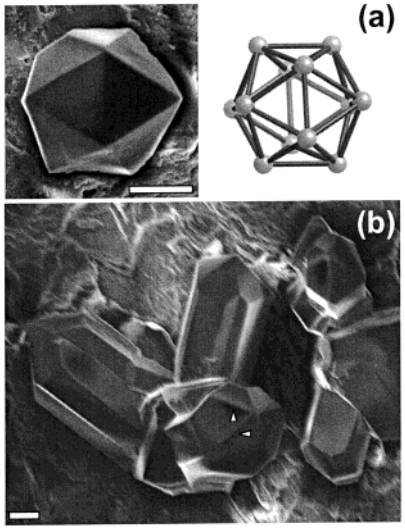


**Figure 4.** Polygonal particles of boron carbide: (a) an icosahedral quasicrystal of boron carbide and the structure model of the $B_{12}$ icosahedral unit; (b) rodlike icosahedra-based particles of boron carbide. Scale bars: 10 $\mu$m.

rather than parallel to the [1,−1,−1] view direction. It will be seen below that the side surface could be the (0,1,2) plane, which is also parallel to the [1,2,−1] elongating direction.

The presently obtained boron carbide product contains a number of particles exhibiting either a perfect icosahedral quaisicrystal morphology (Figure 4a) or a multiply twinned particle (MTP)[11] normally with a rod shape (Figure 4b). These particles have very large sizes. The average diameter reaches over 20 $\mu$m, which could be the largest size ever obtained for boron carbide icosahedral MTP crystals.[12] Here, we suggest the observed particles (under SEM) be icosahedral quasicrystalline because they show exclusively 5-fold symmetry characteristic of an icosohedral geometry. Of course, critical evidence could otherwise be available if an electron diffraction pattern is obtained for an individual particle. Unfortunately, we even failed to observe a certain particle under the transmission electron microscope. This is because the particles are too large, i.e., over 15 $\mu$m, which the carbon foil on the copper grid for TEM observation could not afford. Meanwhile, the size is too large for a possible clear diffraction pattern, considering the poor penetration ability of electron beams. Nevertheless, by referring to similar studies on icosahedral quasicrystals and considering the crystallography of boron carbide,[11−14] we suggest that these specially shaped particles be icosahedral crystals while no other possible structures could be reasonable.

The icosahedral crystals can be considered as a Mackay packing of icosahedral $B_{12}$ units (see structural model in Figure 4a) and thus have long-range order without translational symmetry.[13,14] A rhombohedral (Hex) structure can favor the Mackay packing of 20 tetrahedra because it nearly exactly fits the geometrical requirements in which the tetrahedra are distorted so that the lengths of the edges pointing to the center are slightly smaller than the lengths of the three edges of the outer faces by a factor of 0.951. Then the three triangular side surfaces in the distorted tetrahedron shows an angle (the angle between adjacent 5-fold axes of an icosahedron) of 63.44° rather than 60°. Behind such bonding configuration, a packing density can reach the 0.929 of the maximum.[14] In the rhombohedral (Hex, $R\bar{3}m$) structure of boron carbide, the twin-packed tetrahedra show three equivalent {1,−1,−1} surfaces (or twin planes) and a (0,0,1) surface, which is also the surface of the 20 facets in the composed icosahedra (Figure 5). It can be seen in Figure

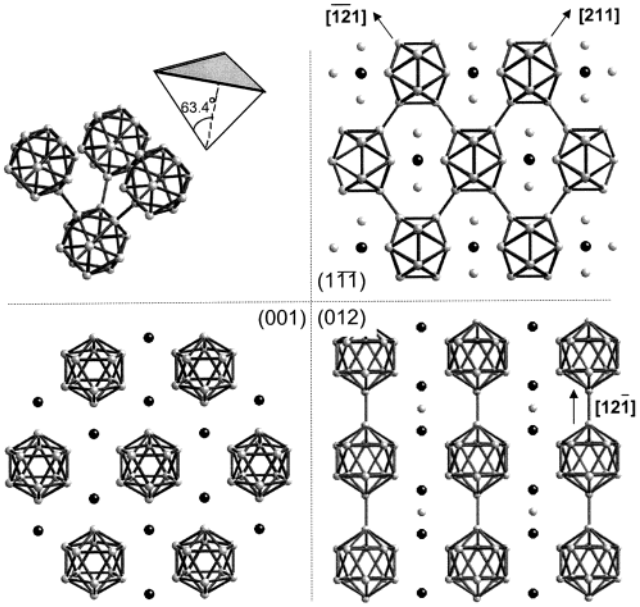


**Figure 5.** $B_4C$-type bonding structures on different crystallographic planes, i.e., (1,−1,−1), (0,0,1), and (0,1,2). The tetrahedron indicates the configuration of $B_{12}$ icosahedra in which the shadowed surface refers to the (0,0,1) plane while the other three facets represent the {1,−1,−1} faces.

5 that the {1,−1,−1} plane shows a two-dimensional bonding network of $B_{12}$ icosahedra. The bonding chains are continuous along two ⟨211⟩ directions. However, no interconnection of icosahedra occurs on the (0,0,1) plane. The closest two B atoms from different icosahedra on the (0,0,1) plane have a distance of 0.274 nm, which is much larger than the bonding length of 0.171 nm on the {1,−1,−1} planes. According to the theory of crystal growth, (0,0,1) facets should not appear in the as-grown crystals. This is why icosahedral particles are usually difficult to be coarsened. Alternatively, truncated icosahedra-based crystals dominate the morphology of boron carbide particles, showing well-developed faces.

In our present work, rodlike crystals involve the majority of the boron carbide particles as shown in Figure 4b. Each rod has a cap showing the pentagonal pyramid morphology, hence a derivative from the icosahedra. The side surfaces of the rods are parallel to the 5-fold axis that is projecting in a ⟨1,2,−1⟩ direction in the $B_4C$ rhombohedral (Hex) structure. Thus, the side surface should be the {0,1,2} planes. The bonding structure on a {0,1,2} plane shows one-dimensional $B_{12}$ chains along ⟨1,2,−1⟩ (Figure 5). This determines the growth habit of a rod shape along ⟨1,2,−1⟩ directions. It seems that the growth morphology is fully determined by the bonding structures in boron carbide, especially for the present case in which no kinematical elements such as metallic catalysts were involved. The {1,−1,−1} faces are the most dominant growth planes that occupy the majority of the crystal facets although most of them become the twin boundaries in MTPs. It is reasonable to consider that {1,−1,−1} surfaces may appear if the synthesis conditions do not favor the formation of twin-related particles. In Figure 4b, we can find some wedge-shaped indents along the rod axis. Additional surfaces are introduced that are parallel to the {1,−1,−1} twin boundaries. These indented rod particles could be the precursors or nuclei of the final nanosheets (see arrowed regions in Figure 4b). Here, we propose a possible formation mechanism for the boron carbide 2D nanostructure, as depicted in Figure 6. The continuous lateral growth of the {1,−1,−1} surfaces initiated from the indented rod particles

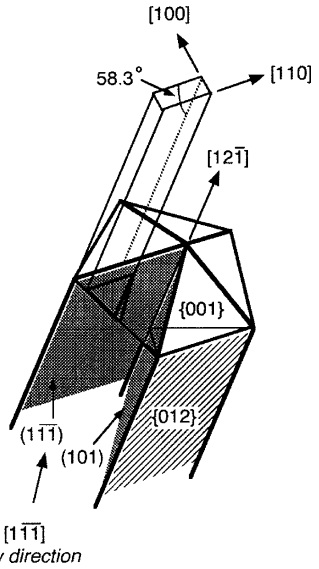


**Figure 6.** Schematic drawing of the geometry of rodlike boron carbide particles, which could be the precursor or nuclei of the final 2D nanomaterials.

gives a platelike morphology. Further thinning of plate thickness is achieved in the later stage of growth. This has been experimentally proved, as pointed out by an arrow in Figure 2a. Then boron carbide 2D nanomaterials appear. The beltlike nanosheet is considered to be bounded by one $\{1,-1,-1\}$ plane (on either side of the lateral sheet), a $\{0,1,2\}$ face at the side surfaces, and a (0,0,1) facet at the top surface. Then the edges of a belt point to the $\langle 1,2,-1\rangle$, $\langle 1,1,0\rangle$, and $\langle 1,0,0\rangle$ directions. The [1,2,−1] and [1,1,0] axes meet at an angle of 58.3°, which is in good agreement with the observed angle in Figure 3a. It seems that the boundary surfaces, or more precisely, the number ($n$) of the different $\{1,-1,-1\}$ surfaces appearing in the growing crystals, dominate the growth morphology. We find that the dimensionality of the product is determined by $(3 - n)$. If the crystallites are bounded by $n = 3$ different $\{1,-1,-1\}$ and one (0,0,1) faces (forming a tetrahedron), icosahedra, the zero-dimensional particles form via self-assembly of the tetrahedra in a multiply twinned fashion. Owing to the difficulty in the lateral growth of the loose-packed (0,0,1) bounding surface (Figure 5), the icosahedral particles are usually small and hard to be coarsened. If the crystallites are bounded by $n = 2$ different $\{1,-1,-1\}$ faces along with $\{0,1,2\}$ and (0,0,1) surfaces, one-dimensional crystallites based on icosahedra morphology, i.e., rodlike MTPs, occur because of a one-dimensional growth habit of $\{0,1,2\}$ facets along the $\langle 1,2,-1\rangle$ rod axis. The existence of two different fast-growing $\{1,-1,-1\}$ surfaces gives a slight two-dimensionality in the directions normal to the rod axis. However, if the crystallites are bounded by only $n = 1$ $\{1,-1,-1\}$ together with $\{0,1,2\}$ and $\{0,0,1\}$ faces, two-dimensional materials, i.e., nanosheets, appear because of the fast lateral growth on the sole $\{1,-1,-1\}$ plane while poor coarsening occurs in the other two dimensions. Again, the one-dimensional growth along [1,2,−1] dominated by the $\{0,1,2\}$ surface and the "zero-dimensional" growth at the tip (0,0,1) surface lead to a beltlike morphology.

The present boron carbide product exhibits a variety of growth morphologies including icosahedra, rodlike MTPs, and mostly beltlike nanosheets. This may imply either a nonhomogeneous synthesis condition, like temperature and/or concentration gradient, within the reaction crucible or changes of chemical environment in the progress of synthesis. The latter effect could more possibly occur in the present small synthesis chamber. Generally, large crystals with unusual 5-fold symmetry are very difficult to achieve. A previous work used a high-temperature, high-pressure technique to obtain $B_6O$ icosahedral particles.[14] For boron carbides, the synthesis conditions seem to be less critical. A simple electric arc discharge technique was reported to synthesize large boron carbide icosahedral crystals (0.5−10 $\mu$m) starting with boron/magnesium powder mixtures.[12] However, the formation mechanism, e.g., the role of magnesium, is not clear. In the present study, no kinematical elements such as metallic catalysts or semiconductor templates were involved in the synthesis of boron carbide crystals. We suggest that the change of vapor pressure during the synthesis at high temperatures could be responsible for the formation of different growth morphologies.

The growth of nanobelts without introducing metal catalysts is likely governed by the VS (vapor−solid) process.[15,16] It seems that surface energy plays a key role in the formation of nanobelt structure.[17] The surface energy is related to the crystal plane; a low-index crystal plane is of lower surface energy. The lower the surface energy, the larger the 2D nucleation probability.[18] On the other hand, an atom absorbed on a low-energy surface has low binding energy and a high probability of desorption. Meanwhile, it has also been indicated that a higher temperature and larger supersaturation ratio facilitate the 2D nucleation, resulting in the formation of the sheetlike structure. In contrast, a lower temperature and smaller supersaturation ratio promote the growth of wirelike structures.[19] The above VS growth kinetics seems to govern the growth morphology of boron carbide crystallites. The previous work in our group employed a lower temperature (1650 °C) and smaller $B_2O_3$/C ratios (from 1:1 to 4:1) and obtained boron carbide nanowires.[10] In the present work, we increased the synthesis temperature (1950 °C) and the starting $B_2O_3$/C ratios by soley using $B_2O_3$ powder whereas a small amount of carbon came from the graphite crucible. Therefore, at the earlier or intermediate stage of synthesis, the high vapor ($B_2O_3$ or BO) pressure along with the extremely high temperatures favor the creation of boron carbide icosahedral crystals via a Mackay stacking. The unstable (0,0,1) surfaces in the icosahedral geometry find thermodynamic supports to exist. At the later stage of synthesis, the continuous expense of $B_2O_3$ starting powders caused a decrease in vapor pressure. A metastable $\{0,1,2\}$ surface occurred instead of the least favorable (0,0,1) surfaces. Then, rodlike and truncated MTPs appeared. With a further decrease in vapor pressure, a sole lateral growth of the most favorable $\{1,-1,-1\}$ surfaces took place while growth of other faces was inhibited, hence, the occurrence of nanosheet morphology.

## Conclusions

We reported the synthesis, structures, and formation mechanism of the boron carbide 2D nanomaterials showing a beltlike morphology with lateral dimensions of 5−10 $\mu$m (in width) and 50−100 $\mu$m (in length), while the thickness is in the nanoscale range (20−100 nm). A simple CVD method was employed in the synthesis starting solely from $B_2O_3$ powder with a chemically and thermally stable insulating template, graphitic boron nitride, in a graphite crucible. The boron carbide products have a uniform $B_4C$ ($R\bar{3}m$) crystal structure with the chemical composition varying by 5−8 for the B/C atomic ratio. The nanosheets exhibit the sheet plane on $\{1,-1,-1\}$, and the side surface exhibits on $\{0,1,2\}$ and the top facet on $\{0,0,1\}$. Crystallographic analysis indicated the dominant role of boundary planes in the determination of

growth morphology. The lateral growth of the only one $\{1,-1,-1\}$ plane leads to the generation of 2D nanomaterials, while the appearance of two different $\{1,-1,-1\}$ surfaces causes one-dimensional growth along the intersection of the two planes. When all three different $\{1,-1,-1\}$ surfaces appear to form a tetrahedron, these tetrahedra may pack in a Mackay fashion to form icosahedral quasicrystals. The surface energy along with the $B_2O_3$ vapor pressure could be the crucial factors determining the growth morphology in a high-temperature deposition. The present investigation may imply an experimental control of growth morphologies for the boron carbide, an outstanding hard material.

## References and Notes

(1) Wood, C.; Emin, D. *Phys. Rev. B* **1984**, *29*, 4582.
(2) Telle, R. In *Structure and Properties of Ceramics, Materials Science and Technology*; VCH: Weinheim, Germany, 1994; Vol. 11.
(3) Sezer, A. O.; Brand, J. I. *Mater. Sci. Eng. B* **2001**, *79*, 191.
(4) Lazzari, R.; Vast, N.; Besson, J. M.; Baroni, S.; Corso, A. Dal. *Phys. Rev. Lett.* **1999**, *83*, 3230.
(5) Zhang, D.; McIlroy, D. N.; Geng, Y.; Norton, M. G. *J. Mater. Sci. Lett.* **1999**, *18*, 349.
(6) McIlroy, D. N.; Zhang, D.; Cohen, R. M.; Wharton, J. *Phys. Rev. B* **1999**, *60*, 4874.
(7) McIlroy, D. N.; Zhang, D.; Kranov, Y.; Norton, M. G. *Appl. Phys. Lett.* **2001**, *79*, 1540.
(8) Pender, M. J.; Sneddon, L. *Chem. Mater.* **2000**, *12*, 280.
(9) Carlsson, M.; García-García, F. J.; Johnsson, M. *J. Cryst. Growth* **2002**, *236*, 366.
(10) Ma, R. Z.; Bando, Y. *Chem. Mater.* **2002**, *14*, 4403.
(11) Marks, L. D. *J. Cryst. Growth* **1983**, *61*, 556.
(12) Wei, B. Q.; Vajtai, R.; Jung, Y. J.; Banhart, F.; Ramanath, G.; Ajayan, P. M. *J. Phys. Chem. B* **2002**, *106*, 5807.
(13) Mackay, A. L. *Acta Crystallogr.* **1962**, *15*, 916.
(14) Hubert, H.; Devouard, B.; Garvie, L. A. J.; O'Keeffe, M.; Buseck, P. R.; Petuskey, W. T.; McMillan, P. F. *Nature* **1998**, *391*, 376.
(15) Yang, P. D.; Lieber, C. M. *J. Mater. Res.* **1997**, *12*, 2981.
(16) Pan, Z. W.; Dai, Z. R.; Wang, Z. L. *Science* **2001**, *291*, 1947.
(17) Dai, Z. R.; Pan, Z. W.; Wang, Z. L. *Solid State Commun.* **2001**, *118*, 351.
(18) Lewis, B. In *Crystal Growth*; Pamplin, B. R., Ed.; Pergamon: Oxford, 1980; pp 23−63.
(19) Dai, Z. R.; Pan, Z. W.; Wang, Z. L. *Adv. Funct. Mater.* **2003**, *13*, 9.